

**SIMULATION OF ORGANIC LIQUID SATURATIONS
USING STYRENE MONOMER AND EPOXY RESIN**

By

William J. Peplinski

John L. Wilson

Steve Conrad

Hydrology Report No. H89-1

(Formerly Open File Report No. 89-1)

NEW MEXICO TECH HYDROLOGY REPORT SERIES

**HYDROLOGY PROGRAM
SOCORRO, NEW MEXICO 87801**

May, 1989

This report was also submitted by William J. Peplinski as an Independent Study in
partial fulfillment of the requirement of the M.S. Degree in Hydrology

Research Sponsored

by:

Environmental Protection Agency

Contract No.: CR-813571-01-0

And

New Mexico Water Resources Research Institute

Contract No. 1345648

ABSTRACT

Bench-top short column experiments were performed with polymers and epoxy resins to visualize non-aqueous phase organic liquid movement and capillary trapping in conditions simulating the saturated and vadose zones. A 3000 ppm CaCl_2 solution and styrene monomer, respectively, modeled the water and organic fluid phases in the saturated zone experiments. The styrene was polymerized and, in some cases, the column was dissected for visual inspection of the organic liquid phase distribution with a scanning electron microscope. Although the technique can be used for any non-wetting fluid saturation, we chose to look only at residual saturations. At residual saturation in the saturated zone the polymerized styrene was disconnected into individual ganglia or blobs. These hardened styrene objects were referred to as 'blob casts'. In other experiments, the water was replaced with dyed Tra-Bond® 2114 epoxy resin, after the styrene had been polymerized. Once the epoxy hardened, the column was cut into sections and examined under an epifluorescent optical microscope. These sections were referred to as 'pore casts'. Heterogeneities were studied by packing a column such that three coarse sand lenses, surrounded by a fine sand matrix, ran parallel to the fluid flow direction. For vadose zone conditions, dyed styrene and two epoxy liquids were sequentially applied, drained, and hardened in an attempt to simulate fluid distributions of water, organic liquid, and air. The resulting pore casts were photographed under an epifluorescent optical microscope.

TABLE OF CONTENTS

ABSTRACT ..	1
TABLE OF CONTENTS ..	2
LIST OF FIGURES ..	3
LIST OF TABLES ..	4
INTRODUCTION ..	5
COLUMN DESIGN ..	6
FLUID AND SOIL CHARACTERIZATION ..	6
Sevilleta Soil ..	8
SATURATED ZONE EXPERIMENTAL PROCEDURE ..	10
Packing and De-gassing ..	10
Styrene Preprocessing ..	13
Styrene Flooding ..	14
Water Flooding ..	16
Styrene Polymerization ..	16
Observation of Styrene Residuals ..	16
VADOSE ZONE EXPERIMENTAL PROCEDURES ..	18
Wetting Phase ..	19
Intermediate Wetting Phase ..	20
Non-Wetting Phase ..	20
EXPERIMENTAL RESULTS AND DISCUSSION ..	22
Microscopic Inspection of Blob Size and Shape in Blob Casts and Pore Casts ...	22
Inspection of Heterogeneous Sand Packs ..	27
Unsaturated Zone Experimental Results ..	29
CONCLUSIONS ..	32
REFERENCES ..	34

LIST OF FIGURES

Figure 1. Exploded view of the TFE Short Column.	7
Figure 2. Viscosity of initiated styrene vs. time.	8
Figure 3. Particle size analysis of sevilleta sand	10
Figure 4. Water saturation of the bottom endcap.	11
Figure 5. Experimental setup of a styrene flood.	14
Figure 6. Intermediate-wetting phase flood.	21
Figure 7. SEM photomicrographs of individual blobs removed from the Sevilleta sand.	23
Figure 8. SEM photomicrographs of more complex blobs. Note that some show signs of breakage.	23
Figure 9. Photomicrograph of Sevilleta sand pore cast covering many pores. The pore cast is magnified 20 times.	24
Figure 10. SEM photomicrograph of many blob casts from the Sevilleta sand.	24
Figure 11. Cross-section of styrene flooding into a water-saturated column with organic wet walls: early time on left, late time on right.	26
Figure 12. Photograph of heterogeneous sand pack. Water was flooded from left to right at a low rate. The core is 5 cm long.	28
Figure 13. Photograph of heterogeneous sand pack. Water was flooded from left to right at a high rate. The core is 5.8 cm long.	28
Figure 15. Photomicrograph of three-phase system. On the overlay 'w' stands for wetting phase, 'I' stands for intermediate wetting, and N stands for the non-wetting phase. Note the well drained pore. Sample is magnified 100 times	30
Figure 14. Photomicrograph of drained wetting and drained intermediate- wetting phases in a glass bead pack. Beads are 1 mm in diameter	30
Figure 16. Schematic cross-section through a coarse grained soil. W stands for the wetting phase; I stands for the intermediate wetting phase; N stands for the non-wetting phase.	32

LIST OF TABLES

Table 1. Properties of fluids used in pore and blob cast visualization experiments. All measurements were taken at 23_C.	9
Table 2. Absolute viscosities of selected organic liquids at 20_C in Centipoise. Data from laboratory measurements and Weast (1986).	15
Table 3. Two-phase TFE column residual saturation results; styrene was used as the non-wetting phase unless otherwise noted.	25

INTRODUCTION

Hydrocarbons and other non-aqueous phase organic liquids make up a large percentage of sub-surface contaminants at leaking underground storage tanks and hazardous waste sites (e.g., Burmaster and Harris, 1982; Chaffee and Weimar, 1983; Convery, 1979; Feenstra and Coburn, 1986; Roberts et al., 1982; Jercinovic, 1984; Maugh, 1979 ; McKee et al., 1972). Usually released at or near the surface, these organic liquid contaminants move downward through the vadose zone toward the water table. As they migrate downward, and after they reach the water table, a portion of the organic liquid is immobilized within the pore space by capillary forces. Although generally regarded as immiscible with water, many organics have aqueous solubilities greater than drinking water standards and in addition have high vapor pressures. Hence even relatively small volumes of organic liquid, trapped in pore spaces, can act as continuing sources of contamination to aquifers and water supplies. In the unsaturated zone, above the water table where pressure heads are less than zero, the organic liquid fills soil pores and covers soil particles in thin films. In the saturated zone, below the water table where water phase pressure heads are greater than zero, the organic phase is trapped in the center of pores as disconnected blobs, or ganglia. This trapped organic phase can remain behind even after a spill site has been cleaned up.

To effectively model this situation requires knowledge of the size, shape, and spatial distribution of the 'blobs', or residual saturation. Residual oil saturation, as the trapped organic phase is referred to in petroleum reservoir engineering, is measured as the volume of organic liquid trapped in the pores relative to the volume of the pores. The technique of using styrene monomer, or epoxy, to represent non-wetting fluids in indurated rocks and glass bead packs has been used previously by petroleum engineers (Morrow, 1984; Yadov et al., 1987; McKeller and Wardlaw, 1988), but so far little work has been done using this technique in unconsolidated soils. Styrene's immiscible behavior with water, its low viscosity, and its ability to harden, or polymerize, while in contact with water make it ideal for simulating non-aqueous phase liquid movement through soils. It can also be used to simulate a low viscosity wetting phase, such as water.

Pore and blob casts were produced for saturated zone conditions, in a homogeneous sand, by a technique in which an organic liquid was solidified in place within a soil column at the conclusion of a displacement experiment, allowing the distribution of organic liquid to be observed. The polymerized organic phase was rigid and chemically resistant. Following polymerization, the solid matrix of the soil column was dissolved with hydrofluoric acid, leaving only the hardened organic liquid, or 'blob cast'. The solidified organic phase was then observed under a scanning electron microscope (SEM) and photographed. Sometimes, instead of dissolving the matrix, the water phase was removed and replaced by an epoxy resin. The solid core, composed of soil, solidified styrene (the organic phase), and epoxy resin (the water phase), was cut into sections to show the organic liquid phase in relation to the soil and the water phase. The sections, or 'pore casts', were photographed under an optical microscope. Although polymerization only gave a 'snapshot' of the displacement process, it offered the advantage of seeing organic liquid in its 'natural habitat', within a soil. Heterogeneous sand packs were also studied. For vadose zone conditions, styrene and epoxy liquids were sequentially applied, drained and hardened in an attempt to simulate proper fluid distributions above the water table.

COLUMN DESIGN

Each of the three columns used to hold the soil sample in the styrene/epoxy resin impregnation experiments were constructed from a 5 cm long tetrafluoroethylene (TFE) cylinder (5 cm I.D., 6.5 cm O.D.), and two aluminum-TFE endcaps with 3000 psi valves. A schematic of a typical TFE column is shown in Figure 1. TFE was chosen for the columns because of its non-reactivity and ease of machining. Both endcaps were made of virgin TFE rod (7.6 cm in diameter, 3.8 cm long) with 0.6 cm thick aluminum plate screwed to the backs. An external groove was cut in the cylinder into which fit a 10 cm diameter aluminum split ring. Four threaded rods passed through the aluminum plates and split ring and provided a means of attaching the endcaps, essentially bolting them on. Four o-rings, one on each end of the cylinder and one on each of the endcaps, securely sealed the column and created a purely mechanical method of holding filters in place.

The inner face of the endcaps had radial and concentric grooves machined into them to allow better fluid flow between the soil sample and the 1/16 inch endcap center hole. In addition, a round fritted glass disc (50 mm diameter, 5 mm thick) was fitted on top of the groove pattern of the lower endcap as a support for filters. Nupro® plug valves were threaded through the aluminum plates and sealed against the TFE rod with Viton® o-rings.

A Magna 66 nylon filter with pore diameters of .22 μm , held in place by an o-ring, was used on the bottom endcap. It acted as a semi-permeable membrane; when water-wet the filter would allow water to pass but not a non-wetting phase, such as styrene. The nylon filter was covered with a paper filter to prevent abrasion against the sand. A paper filter alone was used on the upper endcap to prevent fine soil particles from leaving the column.

In experiments which required epoxy drainage, Millipore's 0.2 μm Durapore® (polyvinylidene difluoride) filters were used in place of the water-wet nylon filters.

FLUID AND SOIL CHARACTERIZATION

Measurements of fluid properties such as viscosity, specific gravity, surface tension, and interfacial tension were performed following procedures outlined by the American Society for Testing and Materials (ASTM, 1986). Viscosity was measured with Cannon-Fenske routine viscometers according to ASTM methods D445-83 and D446-85a. Specific gravity measurements were made as described by ASTM method D1429-76 (pycnometer procedure). An adaptation of ASTM procedures D 1590-60 and D 971-82 were used to determine surface tension and aqueous-organic interfacial tensions, respectively, with a Fisher Manual Model 20 tensiometer.

A 3000 ppm CaCl_2 solution was used as the aqueous phase in all column experiments. Distilled, de-ionized water was de-gassed by boiling. Enough calcium chloride dihydrate was added to the cooled water to bring the concentration to 3000 ppm. The solution was stored under a vacuum to keep it de-gassed. The properties of this aqueous phase are given in Table 1.

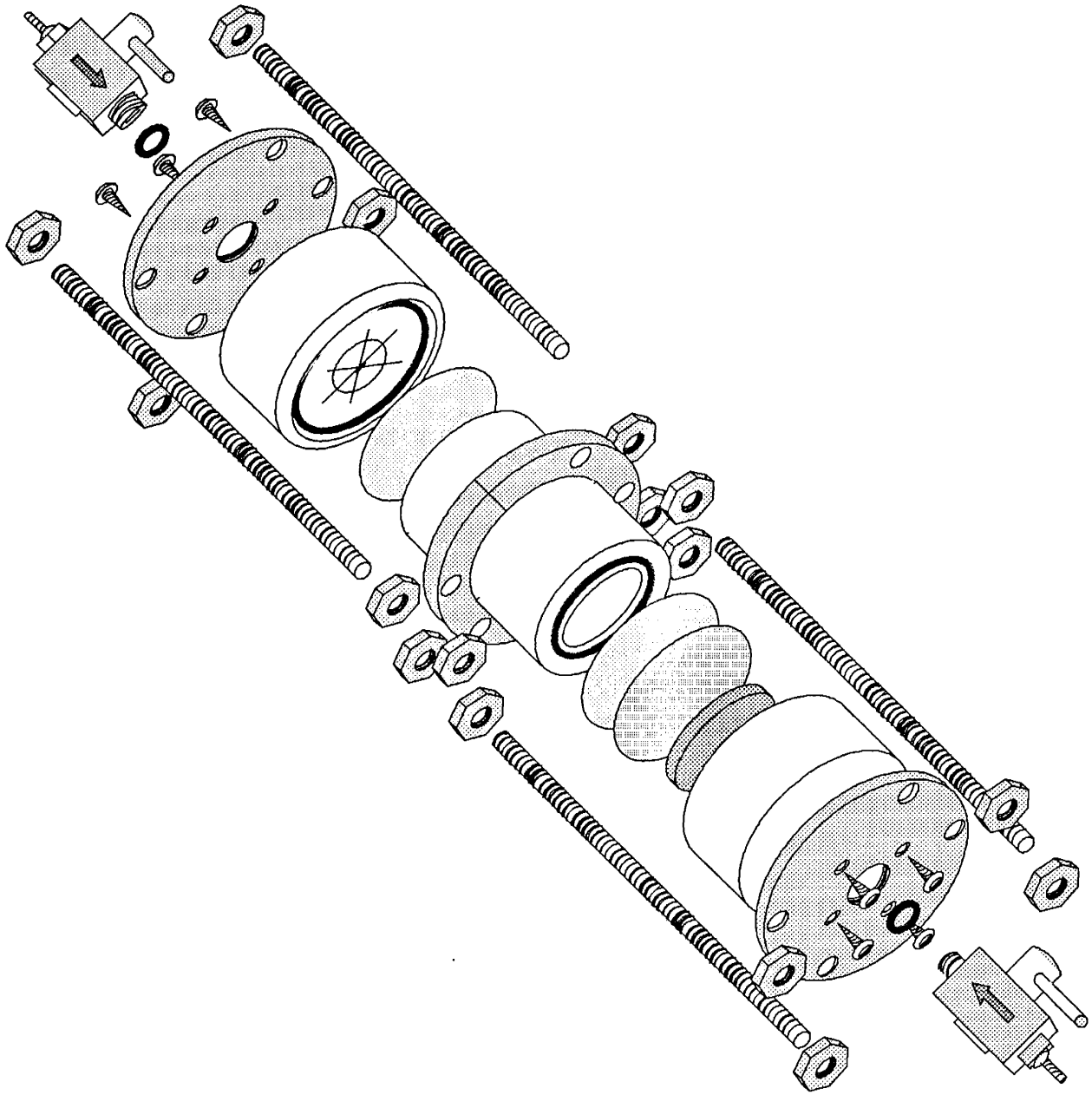


Figure 1. Exploded view of the TFE Short Column.

Although styrene is generally a good model of organic liquids it does have its drawbacks. Styrene has a low viscosity, but once initiated the viscosity increases over time, indicating that polymerization begins as soon as initiator is added (see Figure 2). Styrene also shrinks in volume by roughly 17% (Boyer, 1970) during polymerization. This must be taken into consideration if any optical measurements are to be made. The interfacial tension (IFT) of the styrene with CaCl_2 solution was measured and appeared to remain constant over time ($\sigma_{ow} = 35.3 \pm 0.3$ dynes/cm) even when the benzoyl peroxide initiator was added.

Dyes were added to the styrene in order to improve its visibility, but they changed fluid properties. For example, 9,10-diphenylanthracene (maximum adsorption 260 nm) was added to styrene (0.6% by weight as recommended by McKeller and Wardlaw, 1988) causing the styrene to fluoresce blue under ultraviolet light. Addition of the dye caused the interfacial tension (IFT) with CaCl_2 solution to decrease from $\sigma_{ow} = 35.3 \pm 0.3$ to 30.9 ± 3.0 dynes/cm, and also caused viscosity changes, as shown by Figure 2. Other dyes tried, such as oil blue N (IFT σ_{ow} of styrene + dye = 20.2 ± 0.5 dynes/cm ; surface tension σ_{oa} of styrene + dye = 31.8 ± 0.3 dynes/cm) and phthalocyanine blue did not work well enough to justify further characterization. The blue dyes did not color the styrene deeply enough for it to be visible in small quantities, such as small blobs in pore spaces.

Tracon's Tra-Bond® 2114 epoxy was used in several experiments, in addition to styrene, to represent the wetting or non-wetting phase. Rhodamine B (maximum adsorption 543 nm), a red-orange fluorescent dye, was dissolved in benzyl alcohol and added to the Tra-Bond® 2114 epoxy,

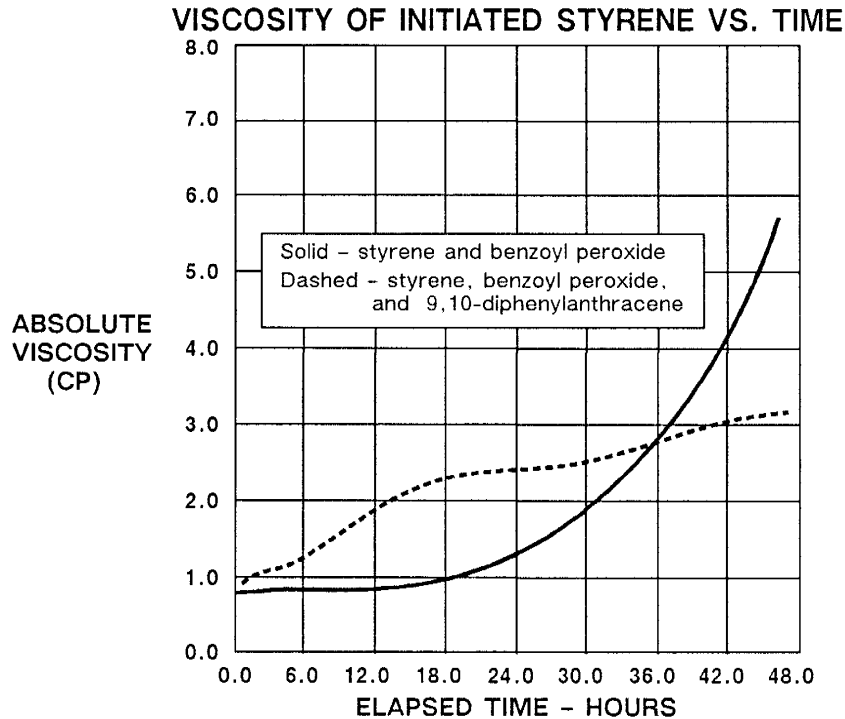


Figure 2. Viscosity of initiated styrene vs. time.

liquid	specific gravity	density (g/cm ³)	kinematic viscosity (cst)	dynamic viscosity (cp)	interfacial tension with 0.3% CaCl ₂ solution (dynes/cm)	surface tension (dynes/cm)
aqueous phase	1.003 ± 0.002	1.000 ± 0.002	0.98 ± 0.01	0.98 ± 0.01	not applicable	72.0 ± 0.4
styrene	0.906 ± 0.002	0.903 ± 0.002	0.89 ± 0.01	0.81 ± 0.01	35.3 ± 0.3	31.9 ± 0.3
Tra-Bond 2114	1.204 (factory)	1.2 (factory)	545 (factory)	597 (factory)	miscible	40.9 ± 0.5

Table 1. Properties of fluids used in pore and blob cast visualization experiments. All measurements were taken at 23°C.

but no characterization was done beyond that stated in Table 1. The benzyl alcohol caused a slight decrease in the resin's viscosity and in its surface tension. In the vadose zone experiments benzyl alcohol (40% by weight) was added to the Tra-Bond resin. This reduced the viscosity to about 50 cps and decreased the surface tension to 38 ± 1 dynes/cm.

Sevilleta Soil

The Sevilleta sand was used in all of the flow visualization experiments. It was obtained locally and has been well studied by researchers at New Mexico Tech. The grains are sub-angular to sub-rounded. A mineral characterization of the sand indicates that it is composed mostly of quartz grains (72 ± 5 % by number), with lesser amounts of feldspar (11 ± 2%) and lithic fragments (16 ± 3%). The lithics were generally much smaller in size than the other mineral grains; they compose about 5% of the sand by volume. When in contact with styrene and water, the sand was wetted by the water. When in contact with styrene and air, the sand was wetted by the styrene. An organic carbon analysis was conducted at North Carolina State University (courtesy of Dr. Cass Miller) and yielded an organic carbon content of 0.02%, an almost negligible amount.

The particle density of this sand was determined to be 2.65 ± 0.02 g/cm from five replicate measurements. Six sieve tests were conducted to measure the particle size distribution of the Sevilleta soil. There was excellent agreement between tests with all curves falling essentially on top of one another. The results of one test are presented in Figure 3. The particle size distribution classifies the soil is a uniform medium grained sand, with a median particle diameter of about 0.3 mm (300 microns) and a uniformity coefficient (d_{60}/d_{10}) of less than 2.

Eleven replicate measurements of water-saturated hydraulic conductivity (K_w) and intrinsic permeability (k) were conducted in a constant head permeameter with the following results:

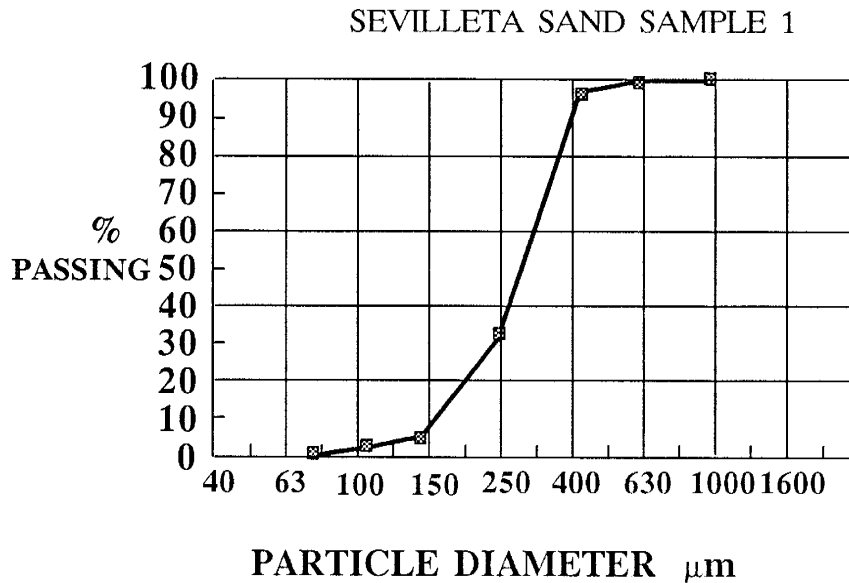


Figure 3. Particle size analysis of sevilleta sand.

$$K_w = (1.03 \pm 0.20) \times 10^{-2} \text{ cm/sec}$$

$$k = 1.03 \times 10^{-7} \text{ cm}^2 = 104 \text{ darcys}$$

The intrinsic permeability was calculated from saturated hydraulic conductivity by:

$$k = \frac{K_w \mu_w}{\rho_w g} \quad (1)$$

where: μ_w = dynamic viscosity of water (0.98 cp)

ρ_w = density of water (0.997 g/cm³)

g = gravitational constant (981 cm/sec²)

SATURATED ZONE EXPERIMENTAL PROCEDURE

Packing and De-gassing

Both homogeneous and heterogeneous sand-pack experiments were performed in the TFE columns. The packing and degassing procedures for the homogeneous case are reviewed first, followed by the heterogeneous case. Equations are then presented for calculating pore volume, bulk density, and bulk porosity, after packing.

Before packing a column with soil to be used in a homogeneous saturated zone experiment, the lower endcap with filters was tightly bolted to the TFE cylinder, and the cylinder and endcap were attached to an 18 cm Hg vacuum. Then the column was inverted and placed in a large beaker of CaCl_2 solution. Liquid was drawn through the filters, fritted glass disc, and associated plumbing to saturate them with water (see Figure 4). When air bubbles were no longer observed, the column was removed from the vacuum and the filters checked visually for integrity. The water wet filters should have prevented the flow of the non-wetting air phase. If the filters did not allow air flow the whole column was dried and weighed. This was called the empty column weight, M_e . Mettler PE1600 and PM11 scales, with 1600 ± 0.01 gram and 11000 ± 0.1 gram capacities respectively, were used for the gravimetric measurements in these experiments.

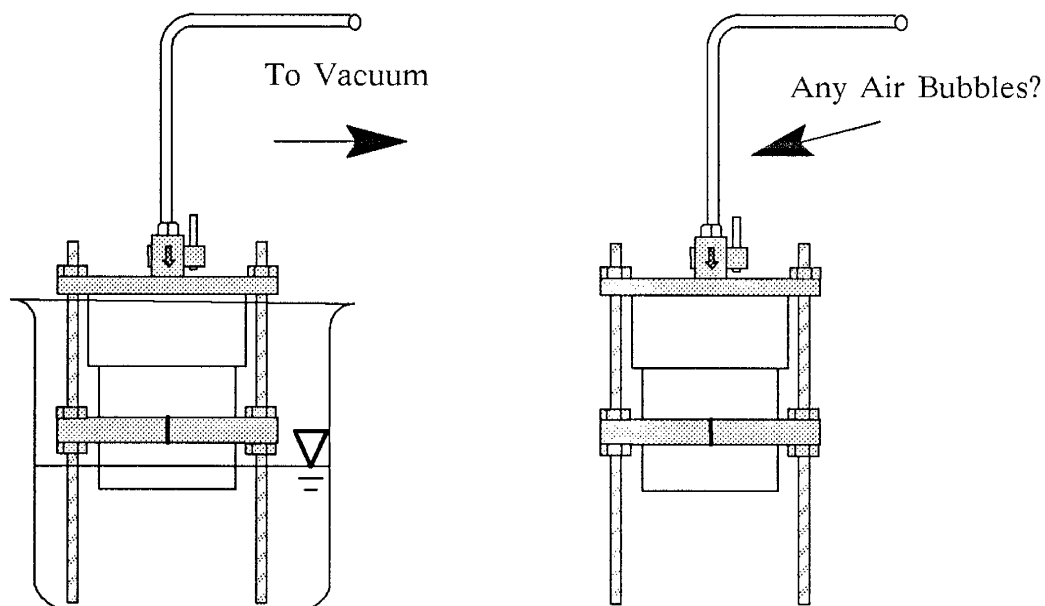


Figure 4. Water saturation of the bottom endcap.

Next, a buret filled with CaCl_2 solution was attached to the bottom endcap and the solution was allowed to fill the column to a depth of 2 cm. Oven dried Sevilleta sand, which had been weighed previously, was then poured and packed into the column, taking care to keep the packing surface below the solution surface. Lab spatulas, bent to a 90 degree angle, were used to pack the soil down. The process of filling the column with CaCl_2 solution and then packing soil was repeated until the solution level was approximately 2 cm from the top of the cylinder. At that point capillary rise of the solution was used to saturate the soil/sand as much as possible, since there was nothing to prevent overflow of liquid from the column. Sand packed above the end of the cylinder was carefully scraped off with a lab spatula and collected together with spilled sand. After drying, it was combined with unused sand. The mass of soil in the column, M_s , was simply the difference between the initial soil mass minus any leftover. O-rings and a paper filter were placed on the cylinder to seal and prevent the

escape of clays and other fines, respectively, and the upper endcap was lowered onto the column and bolted on.

Some trapped air remained on or between soil particles, especially near the top of the column, and had to be removed. Flooding the column with 25 pore volumes (~800 ml) of de-gassed CaCl_2 solution usually solubilized the trapped air and removed it from the column. The solution was introduced through the bottom endcap and out the top endcap. Periodic gravimetric measurement of the column was used to determine whether or not an equilibrium had been established. When the column reached equilibrium all the entrapped air had been removed from the column and the plumbing. The equilibrium mass was called M_1 .

The heterogeneous sand pack column experiments were performed using the Sevilleta sand, split with a size 50 sieve (≈ 296 microns) into coarse and fine portions, approximately 45% and 55% by mass, respectively. The finer fraction was used as a matrix to surround 3 stringers or lenses, composed of the coarser fraction. The stringers were roughly circular in cross-section.

The major difference in packing technique between the homogeneous and the heterogeneous cases was that the heterogeneous columns were packed dry. The TFE cylinder and water saturated bottom endcap were assembled as described earlier, in the homogeneous packing procedures, but no CaCl_2 solution was allowed to flow into the column while it was being packed. This was to preserve the paper forms which were used to separate the coarse stringers from the fine sand. The three paper cylinders were constructed with diameters calculated so that the sum of their cross-sectional areas would equal approximately 45% of the cross-sectional area of the column. This was done so that any given cross-section would roughly have the same percentage of grain sizes as a cross-section through a homogeneous column.

A 6 to 7 mm thick layer of the fine sand was placed on the bottom of the column assembly and the paper cylinders were pushed down into it. This held the forms upright. Then the fine sand was carefully poured and packed around the forms, so as not to collapse them, until the level of the sand was 3/4's of the way to the top of the column. At that point the coarse sand was packed, using a lab spatula, into the paper cylinders. They were filled to approximately 6 to 7mm from the top of the column. The rest of the matrix was then filled with the fine sand. The three paper forms were slowly pulled out of the column and any remaining volume was filled with the fine sand. CaCl_2 solution was then pushed upwards, through the bottom endcap, wetting the sand. Settling of the sand was observed, and more fine sand was added to the top of the column. When the sand-pack was totally wetted, excess sand was removed from the top of the column and the upper endcap was attached, as described earlier.

Degassed CaCl_2 solution was flooded through the column until a gravimetric equilibrium was attained. The mass of water in both the homogeneous and heterogeneous columns was determined from:

$$M_w = M_1 - M_e - M_s \quad (2)$$

where: M_w = mass of water in the column (g)
 M_1 = de-gassed, water saturated, sand packed column mass (g)
 M_e = mass of the empty column (g)
 M_s = mass of soil in the column (g)

Estimates for pore volume, soil volume and total effective column volume were also calculated from these gravimetric measurements:

$$V_p = \frac{M_w}{\rho_w} \quad (3)$$

$$V_s = \frac{M_s}{\rho_s} \quad (4)$$

$$V_T = V_p + V_s \quad (5)$$

where: V_p = pore volume of the column (cm³)
 V_s = volume of soil sample in the column (cm³)
 V_T = total volume of the column (cm³)
 ρ_w = density of water (g/cm³)
 ρ_s = particle density (g/cm³)

Finally, the bulk density, ρ_b , and bulk porosity, n , of the soil pack were determined:

$$\rho_b = \frac{M_s}{V_T} \quad (6)$$

$$n = 1 - \frac{M_s}{\rho_s V_{ce}} \quad (7)$$

where: M_s = mass of soil in the column (g)
 ρ_s = particle density of the soil (g/cm³)

Styrene Preprocessing

Styrene monomer is commonly sold containing an inhibitor to prevent polymerization during transport and storage. Distillation of styrene has been the preferred method to remove the inhibitor, but the distillation process is quite involved due to styrene's volatility. In order to simplify the laboratory procedure, inhibitor removal columns developed by Aldrich Chemical Company (cat.# 30,632-0) were used to remove the 4-tert-butylcatechol inhibitor from the styrene.

Inhibited styrene, held in a separatory funnel, was slowly dripped into the column and then collected in a beaker or flask at the bottom of the column. Each inhibitor removal column has the

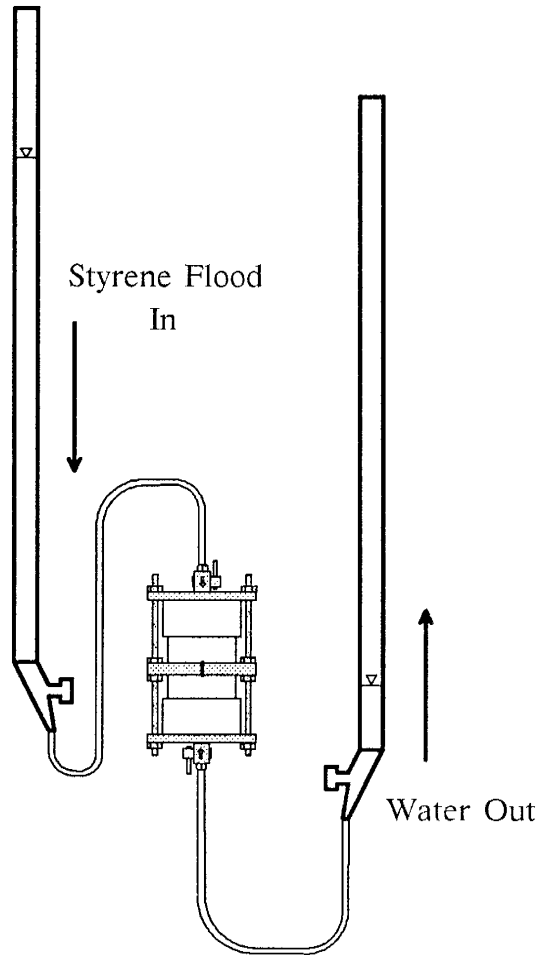


Figure 5. Experimental setup of a styrene flood.

capacity to remove inhibitor, at 15 ppm, from up to 4 liters of styrene. The uninhibited styrene was weighed and benzoyl peroxide, 1% by weight, was added as an initiator. Benzoyl peroxide was chosen as an initiator because it was found to preserve the water wetness of the soil sample (Chatzis et al., 1984). Dyes were then added to the styrene.

Styrene Flooding

The initiated, dyed styrene was transferred from the flask to a 100 ml buret which was attached to the upper endcap of the de-gassed column. The styrene was elevated to a head of approximately 1 meter above the column. Valves on the water and styrene burets, and those on the column, were opened and styrene flowed into the column, as illustrated in Figure 5. During the flooding, the head on the column decreased as styrene left the buret. Head drops of 30 to 40 cm, depending on the column,

benzene	0.65
toluene	0.59
m-xylene	0.62
gasoline	0.48
soltrol-130	1.45
kerosene	1.73

Table 2. Absolute viscosities of selected organic liquids at 20° C in Centipoise. Data from laboratory measurements and Weast (1986).

were common. Water, displaced by the styrene, passed through the nylon filter and left the column via the lower endcap. Water entering the outflow buret caused an increase of head on the lower endcap and slowed the flood.

Experiments with the organic liquid Soltrol-130, an isoparaffinic solvent, have shown that the column-buret system required close to 48 hours before residual or irreducible water saturation (S_{wr} or S_{wi}) was reached. The time dependent nature of styrene's viscosity, however, required the experiment to be completed within 24 hours of initiation. Experiments running longer would be of questionable value since the viscosity would be increasing. Besides, many organic liquids of interest generally have viscosities close to that of water (see Table 2). Attempting to displace a more viscous fluid with a less viscous fluid (i.e., displacing viscous styrene with less viscous water) can lead to results different from those obtained from a displacement experiment where the ratio of viscosities is near one. The ratio of the non-wetting fluid viscosity to the wetting fluid viscosity is often referred to as the 'mobility ratio' in petroleum reservoir engineering. High, or adverse, mobility ratios can lead to increased trapping of the non-wetting phase in saturated zone experiments due to viscous instabilities.

After 18 hours the valves on the burets and column were closed. The outflow tubing and buret were checked to see that no styrene was produced. Styrene in the outflow line indicated a leak in the filter which would invalidate the experiment. If none was found the tubing was carefully removed and the column was weighed. This mass was recorded as M_2 . The fluid saturations were calculated as:

$$S_o = \frac{M_1 - M_2}{\Delta \rho V_p} \quad (8)$$

$$S_w = 1 - S_o \quad (9)$$

where: S_o = oil saturation (%)
 S_w = water saturation (%)
 V_p = pore volume (g/cm³)
 $\Delta \rho$ = density difference between fluids (g/cm³)

Organic saturations, S_o , using styrene commonly reached values of $70 \pm 6\%$.

Water Flooding

Styrene was drained from its buret and the other buret was filled with de-gassed CaCl_2 solution. The column, at initial organic saturation, was re-attached to the two burets, the water buret to the lower endcap and the styrene buret to the upper endcap. The CaCl_2 solution buret was raised to a head of approximately 1 meter above the center of the column and all the valves in the system were opened.

CaCl_2 solution entered the lower endcap and flowed upward, displacing the less dense styrene. Connected, or continuous styrene, left the column and no water was produced until approximately 60-70% of a pore volume had passed. For a relatively short period of time after water breakthrough occurred, both styrene and water were produced from the column. A total of 6-7 pore volumes of CaCl_2 solution were flushed through the column in order to ensure equilibrium between the aqueous phase and the organic residual.

The burets were disconnected from the column, as described above, and the column was weighed again. This mass was recorded as M_3 . The residual organic saturation was then calculated as

$$S_{or} = \frac{M_1 - M_3}{\Delta \rho V_p} \quad (10)$$

Observed residual styrene saturations for the Sevilleta sand, following this procedure, were generally $15 \pm 7\%$.

Styrene Polymerization

The styrene residuals were hardened by placing the column in a pressure vessel, pressurizing it to 80 psig and then heating the vessel at 85 degrees centigrade for 40 hours.

The pressure vessel was a 40 cm tall aluminum cylinder (I.D. 10 cm) with 1.3 cm thick walls. The bottom was sealed with a flanged aluminum plate welded to the outer wall. The top was sealed with an o-ring held between the top cap and the face by 10 threaded studs set into the cylinder face. A Nupro® plug valve, with associated fittings, was threaded into the top cap.

Eight hundred ml of de-gassed CaCl_2 solution were poured into the vessel. The column was placed into the pressure vessel with the valves on both ends open and enough CaCl_2 solution was added to cover the column with liquid. The liquid acted to prevent nitrogen from entering the sand pack and also as a diffusion barrier for any oxygen that may be present in the vessel atmosphere.

After the column was sealed into the pressure vessel, a 60 cm Hg vacuum was applied to the head space to evacuate as much atmosphere as possible, then a dry nitrogen source was connected to the plug valve and the vessel was pressurized to 80 psig. Then the vessel was placed in a laboratory oven and heated.

Observation of Styrene Residuals

To complete the saturated zone simulation, either the styrene blobs were removed from the sand matrix or the water/wetting phase was replaced by an epoxy. The first method produced individual

styrene residual 'blob casts', whose shapes and sizes were viewed optically or with a scanning electron microscope. The second method yielded polished epoxy slabs, the 'pore casts', in which the relationships between soil grains, the wetting phase, and the non-wetting phase were studied.

The styrene blob casts were removed from the matrix by dissolving the sand grains with acids. A small portion of the styrene-sand pack was carefully removed from the column with a spatula, placed in a TFE beaker, and dried. The dry sample was covered with one of several concentrated acids and allowed to dissolve for several days after which the sample was filtered through a TFE filter, washed with water, and covered with another acid. This process was repeated with concentrated hydrofluoric acid, sulfuric acid, nitric acid, hydrochloric acid, phosphoric acid, and chromic acid. This combination of acids dissolved essentially all of the matrix and left the resistant styrene blob casts, as well as some insoluble inorganic residue. Several styrene blob casts, as photographed with a scanning electron microscope, are shown later in Figures 7 and 8.

Initially, it was hoped that a large number of the blob casts could be statistically analyzed to determine the size and shape distribution of the residual organic saturation. Although the styrene blob casts were chemically resistant, they were quite brittle and fragile. The transfer of a blob from filter paper to a microscope slide for observation often resulted in the breakage of the blob. It was not clear that the blob casts recovered from the acid bath were wholly unbroken. For this reason, it was decided not to conduct the statistical study as part of this research project.

To construct the pore casts, the column was taken out of the pressure vessel and the top endcap was removed. The column and endcap were placed back in the oven at 75-80 degrees centigrade and allowed to dry for 48 hours. The dried column was reassembled and attached to a pressure vessel filled with rhodamine B dyed Tra-Bond® 2114 epoxy resin. Resin was forced through the soil sample from the bottom of the column with air pressure. Four or five pore volumes of resin were forced through the column in order to remove as much air as possible. Time was of the essence, since when dealing with the Tra-Bond epoxy as it would generally harden within 1 hour, depending on the mix of resin to hardener. Twenty-four hours were allowed for the Tra-Bond epoxy to properly set. The consolidated core was then removed from the column by cutting longitudinally through the teflon sleeve in two spots, and peeling the teflon away.

Rock saws owned by the New Mexico Bureau of Mines and Mineral Resources were used to section the core into 6 or 7 approximately seven mm thick discs. One face on each disc was covered with a thin layer of undyed Tra-Bond 2114 epoxy to fill in holes left by plucked grains, and create a solid surface for polishing. To remove air bubbles trapped under the epoxy, each disc was placed in a vacuum dessicator for 5 minutes under a 60 cm Hg vacuum. When the epoxy layer dried, the disc was cut on a Bureau of Mines trim saw into 9 pieces: 8 edge pieces and one rectangular middle piece. The smaller pieces were easier to polish and hence provided better optical surfaces. Lap (grinding) wheels were used to grind the epoxy layer down to a flat surface. Two-hundred-twenty and 400 grit powders were used to remove the majority of the epoxy coating, and 10 minutes of polishing with 14.5 μm and 9.5 μm grit provided the final surface.

Photomicrography was performed using one of the two in-lab Zeiss SR stereoscopes, or New Mexico Tech's Petroleum Recovery Research Center's Nikon Opti-Phot epifluorescent microscope system. A photomicrograph of a pore cast is shown later in Figure 9.

VADOSE ZONE EXPERIMENTAL PROCEDURES

Attempting to simulate organic liquid transport in the vadose zone using styrene and epoxies presented several difficulties. In the vadose zone, there are three fluid phases: water, air, and the organic liquid. In these visualization experiments, all three phases obviously could not be fluid simultaneously since most epoxies and styrene monomer are miscible. It was decided to simulate the three fluid phases by a sequence of two phase experiments in which the wetting phase of each experiment would be hardened. Styrene was used as the first wetting phase, and nitrogen was used to drain the styrene to a wetting phase residual saturation. Assuming this saturation would not change with the presence of an intermediate wetting phase, the styrene was hardened. Epoxy was then flooded into the column and drained with gas to simulate the intermediate wetting phase. The remaining void space was filled with a second epoxy to simulate the gas phase.

This approach raised a question about wettability and surface energies. Would differences between solid-liquid wetting relationships and the liquid-liquid spreading coefficients cause serious differences between the simulation and reality? The spreading coefficient of fluid X spreading over fluid Y, $S_{X/Y}$, is defined as $\sigma_{ya} - \sigma_{xa} - \sigma_{xy}$. It is the difference between the work of adhesion of X to Y and the work of cohesion of X (Adamson, 1982). The interplay of these same forces in a solid-liquid system characterizes the wettability of that system. Differences between wettability and the spreading coefficient then, arise from the fact that (1) a solid surface will not be deformed by a fluid contacting it, as a liquid interface could be, and (2) in liquid-liquid systems each fluid will partition into the other which causes changes in σ_{xy} over time. In using this method we had to make two assumptions to compensate for these differences: a fluid at a residual wetting saturation is immobile and any deformation caused by another fluid flowing over it is negligible, and we were modeling fluids in which cosolvency effects are negligible. The second assumption is weak in that essentially all organic chemicals of interest are at least slightly soluble in water, and some, benzene for example, exhibit strong cosolvency effects with water.

In this simulation the styrene, acting as a wetting phase, was drained to some residual saturation and hardened. The next intermediate-wetting phase, epoxy, interacted with the immobile 'wetting phase' as it was flooded through the column and subsequently drained. In order to decrease the surface energy of the system, the second phase should have spread out in a thin film over the wetting phase whether the 'wetting phase' is solid or liquid. In liquid-liquid systems it is common that a fluid with a low surface tension, such as a hydrocarbon, covers a fluid with a high surface tension, such as water (Adamson, 1982). The system will exist as a thin film of the wetting phase between the solid surface and the intermediate or non-wetting phase. So in this sense, a solidified wetting phase at residual saturation may be a reasonable approximation of a fluid wetting phase, as long as flow in the wetting phase is not significant (Amaufule and Handy, 1982). Granted, the differences between a

liquid propagating over a solid surface versus a liquid surface, as mentioned above, may affect the experiment but the final results should be similar: a minimization of surface energy.

Wetting Phase

Initially, due to its excellent wetting characteristics, styrene was chosen to represent the wetting/aqueous phase. A column was packed with Seville sand, under dyed initiated styrene, following procedures described previously in the saturated zone methods. Then it was drained with air. Polymerization of the styrene failed, however, because of the air in the sand pack. Oxygen in the air attached to the free radical chain of the styrene, effectively stopping the polymerization process. The sand pack was left as a gooey, viscous mess.

A glove bag was purchased, inside of which a column could be packed in a nitrogen atmosphere. The inert nitrogen atmosphere made it possible for the styrene chains to polymerize unhindered by oxygen molecules. The glove bag was connected to a tank of dry nitrogen, inflated, and purged to remove any air. A vacuum line, with a reservoir outside the bag to collect styrene and tubing attached to a buret were punched through the side of the bag. With these lines, styrene could be removed from, or introduced into, the bag.

Using the vacuum line, styrene was pulled through the bottom endcap of the column to remove atmosphere from behind the nylon filter. Styrene, which had passed from the column to the vacuum reservoir, was transferred to the buret, which in turn was attached to the lower endcap of the column. This source of styrene was used to pack the column in a method similar to that described earlier, for the saturated zone TFE column.

After the packing of the column was completed, a paper filter was placed over the sand and the upper endcap was bolted on. Approximately five pore volumes of styrene were pushed from the buret upward through the column and out to the vacuum reservoir. Nitrogen trapped in the sand pack was removed in this manner. The hydraulic gradient between the buret and the reservoir provided the impetus for styrene flow, so the vacuum was not used. After the styrene flooding, the column was considered saturated. The term 'considered saturated' is used because no gravimetric measurements were made to determine if an equilibrium was attained. Nitrogen may still have been present within the the sand pack or in the lower endcap, but costs of styrene and dye prevented a more thorough de-gassing procedure.

Draining the column to a residual wetting phase saturation was done by applying tension to the sand pack by lowering the styrene buret below the column. Still within the glovebag, the vacuum line was removed from the upper endcap. Styrene drained through the nylon filter to the buret while nitrogen entered the column through the upper endcap. Initially, the styrene-air interface was lowered to 50 cm below the column, and the column allowed to equilibrate. After 1 hour, the buret was lowered another 25 cm and allowed to equilibrate for 2 hours.

The residual styrene was polymerized following the method described in the saturated zone experiment. A difference in procedure to note is that the column was placed into the pressure vessel

while still within the glovebag, so that the nitrogen atmosphere was maintained. Also, no water was present within the pressure vessel in which to submerge the column, only nitrogen gas.

Intermediate Wetting Phase

In most experiments, after the styrene had been polymerized, the TFE column was disassembled and cleaned. Hardened wetting-phase styrene clogged the fritted glass disc, froze the plug valves, and filled the grooves in the endcaps. Soaking the valves and endcaps in toluene dissolved the styrene. The fritted glass disc was discarded. A new fritted glass disc and new filters were used to reassemble the column. Millipore's 0.2 μm Durapore® (polyvinylidene difluoride) filter, with a water-wet air entry value of 50 psig, was used on the lower endcap to drain the epoxy. Durapore filters provided good, although not perfect, epoxy drainage.

Tra-Bond® 2114 resin with rhodamine B dye, 0.5% by weight, and benzyl alcohol, 40% by weight, was pulled under a vacuum into a small stainless steel pressure cylinder. The upper end of the cylinder was removed from the vacuum and reattached to a source of dry air with a pressure of 40 psig. The lower end of the pressure cylinder was connected with tubing to the bottom end of the reassembled column, as shown in Figure 6. A short length of tubing led from the upper endcap of the column to a drainage beaker. The applied air pressure forced resin upwards through the lower endcap displacing air. Approximately one pore volume of the moderately viscous resin was forced through the column in a 45 minute period.

Draining the column was accomplished by turning off the air source, removing the upper drain tubing, and attaching a vacuum line to the pressure cylinder. Thirty cm Hg of tension were applied to the column and this drained approximately 50% of the intermediate-wetting phase volume. The column was allowed to drain until the excess resin in the drainage beaker showed signs of hardening. This was about 1 hour after the hardener was added to the resin. At that time, the valves on the column were closed and the pressure cylinder was disconnected from the system. As the hardening time of an epoxy is dependent on the volume of the epoxy, the fluid within the column was still semi-liquid when the tension was removed.

It took 24 hours for the epoxy to cure after which the column was disassembled and cleaned. Benzyl alcohol was used to flush epoxy from the pressure bottle and to dissolve epoxy from within the endcaps.

Non-Wetting Phase

The third fluid phase to be added to the column represented the non-wetting air phase. Again Tra-Bond® 2114 epoxy was used, but this time it was dyed with coumarin 6. As no drainage of the third phase was required, this step was the easiest of all. The dyed epoxy was pulled into the stainless steel pressure cylinder, as described earlier, and flooded into the column through the bottom endcap. After breakthrough occurred, the excess resin was collected in a beaker and discarded. Forty-eight hours were required for the epoxy to cure.

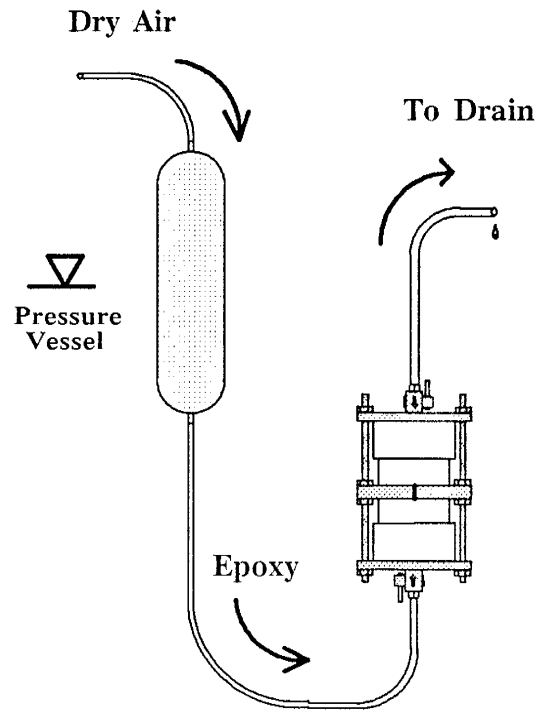


Figure 6. Intermediate-wetting phase flood.

When the core had cured sufficiently, the teflon cylinder was cut away and the core was prepared for observation as 'pore casts', as described previously for the saturated zone experiments.

EXPERIMENTAL RESULTS AND DISCUSSION

Microscopic Inspection of Blob Size and Shape in Blob Casts and Pore Casts

SEM photomicrographs providing a three-dimensional view of polymerized 'blob casts' from a Sevilleta soil column are shown in Figure 7 and 8. The rough spots on the surface of these blobs is probably due to the SEM coating process. There is a typical singlet (upper left), and a doublet (lower left). The singlet is almost spheroidal, with a length of 200 microns and a diameter of 100 or more microns. The doublet includes one pore body of roughly 100 microns in diameter, and another that appears to be almost 200 microns in diameter. At the pore throat, the doublet is only 20 microns in diameter. The two more complex shapes involve four (upper right) and six (lower right) pore bodies. The pore bodies of these more complex blob shapes appear to have a diameter of roughly 100 microns, while the typical throat diameter is less than 50 microns. Contrast these diameters with the grain size distribution of the very uniform Sevilleta soil, as given in Figure 3. The mean grain diameter is 300 microns. Few grains are larger than 500 microns, or smaller than 100 microns. The typical pore body blob diameter of 100 microns is smaller than the mean grain size. The blob lengths depend on the number of pore bodies involved. The singlet in Figure 7 is 200 microns long, the doublet bends through a length of 400 microns, the quadruplet is 800 microns long, and the contorted sextuplet is at least 800 microns long (part of the sextuplet is sticking up into the photo, and thus its entire length is not readily apparent). Several more complex blob casts, taken from the same column, are shown in Figure 8. Here are branched blobs, often with holes in them and 10 or more pore bodies. Presumably, the larger holes were partially filled with a sand grain when in the column. Perhaps the smaller holes contained only the 'pointed edge' of a grain.

The five homogeneous two-phase experiments (Table 3) were performed using the Sevilleta soil and styrene. The S_{or} data set has an average value of 0.16 and a standard deviation of 0.04. Although much care was taken to obtain accurate results, it is obvious from a brief inspection of the error associated with each measurement, that this experimental apparatus should be used for flow visualization and not residual saturation quantification in soils.

Perhaps the largest source of error in the styrene experiments was the mass of the TFE column itself, 1400 grams. It had to be weighed, during the gravimetric determinations of saturation, on a high capacity Mettler PM 11 balance, which has an accuracy of 0.1 grams. Measurement errors (0.1 g) were propagated through the calculations of fluid saturation presented earlier (eqn. 2-10). The error propagation method applied treated the measurement error as a fraction of the measured value. The magnitude of the fraction was always positive, leading to a large cumulative error. That is to say, the errors did not cancel each other out. This method yields, in a sense, the worst possible error. From this it is obvious that the relatively low accuracy of the scale led to a much larger error, associated with each saturation value, than was desirable. The use of a scale with a higher accuracy would perhaps eliminate this problem.

Comparison of these results with results of other in-house experiments indicate that these results are also much lower than expected. Experiments performed in glass chromatographic columns, using

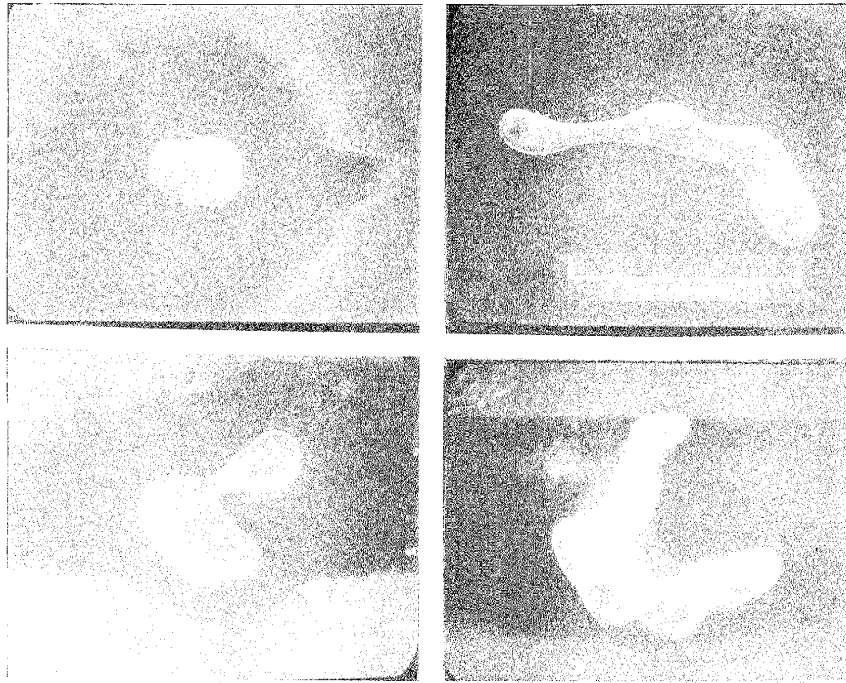


Figure 7. SEM photomicrographs of individual blobs removed from the Sevilleta sand.

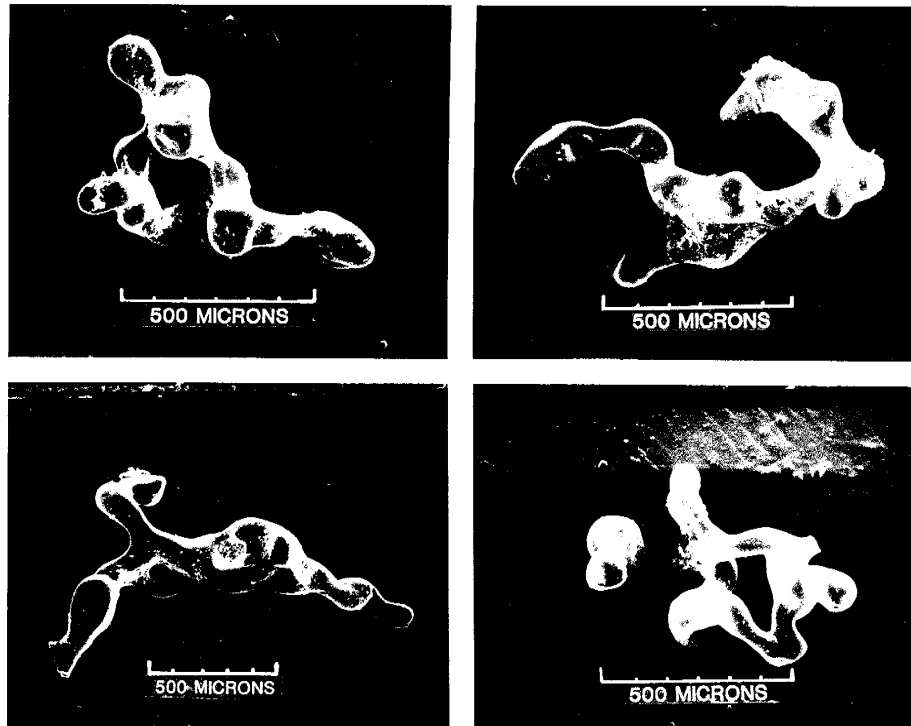


Figure 8. SEM photomicrographs of more complex blobs. Note that some show signs of breakage.

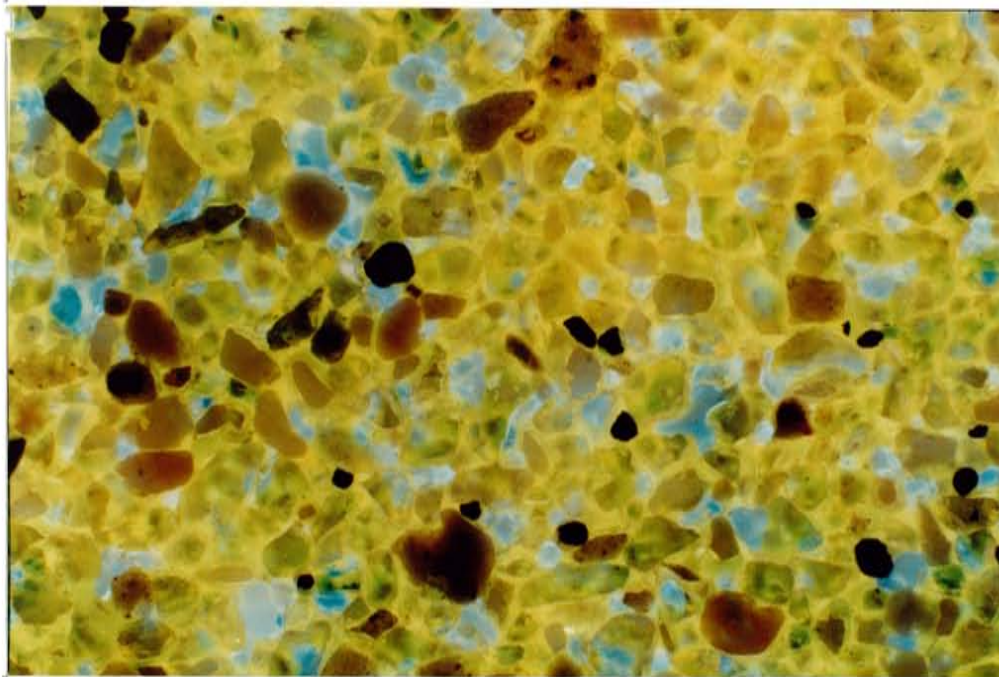


Figure 9. Photomicrograph of Sevilleta sand pore cast covering many pores. The pore cast is magnified 20 times.

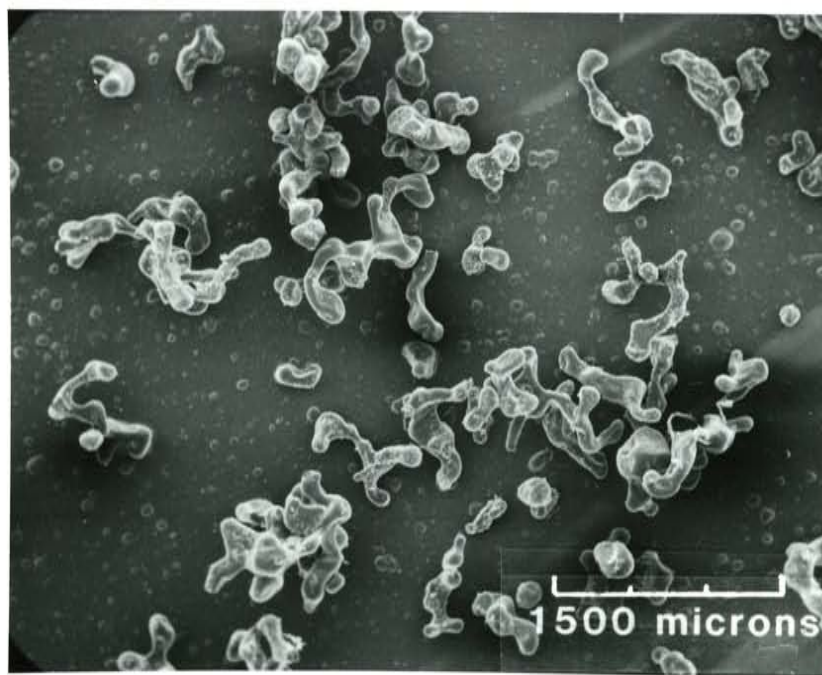


Figure 10. SEM photomicrograph of many blob casts from the Sevilleta sand.

Column	Porosity (%)	S_o	S_{or}
1 homogeneous	32.3	$0.710 \pm .091$	$0.170 \pm .065$
2 homogeneous	33.5	$0.667 \pm .087$	$0.108 \pm .059$
3 homogeneous	33.5	$0.713 \pm .094$	$0.192 \pm .065$
4 homogeneous	31.7	$0.722 \pm .101$	$0.157 \pm .071$
5 homogeneous	34.6	$0.700 \pm .086$	$0.200 \pm .060$
1 soltrol-130	33.4	$0.764 \pm .039$	$0.265 \pm .027$
2 soltrol-130	34.1	$0.745 \pm .038$	$0.186 \pm .025$
1 heterogeneous	37.1	$0.896 \pm .133$	$0.407 \pm .105$
2 heterogeneous	34.5	$0.936 \pm .107$	$0.263 \pm .072$

Table 3. Two-phase TFE column residual saturation results; styrene was used as the non-wetting phase unless otherwise noted. Error bars were calculated to give the worst possible error.

the Sevilleta soil and Soltrol-130 yielded an average S_o value of 85% and an average S_{or} value near 27% (Wilson et al., 1989). We hypothesized that time constraints, put on the experiment by styrene's ever increasing viscosity, did not allow enough time for the column to come to an equilibrium condition during the styrene flood. Therefore, the maximum organic saturations and residual organic saturations were consistently lower than those obtained in similar experiments using the Soltrol-130.

Several experiments were performed to investigate the effect of non-equilibrium flooding. In one experiment Soltrol-130 was flooded into, and drained out of, a TFE column following procedures dictated by the viscosity time constraints of the styrene procedure. The residual saturation obtained matched those commonly found when performing experiments with styrene in the TFE column (19%; see Table 3). Another experiment was performed using Soltrol-130 in the TFE column but followed procedures which allowed sufficient time for the system to reach equilibrium. This experiment produced a value of residual saturation (27%; see Table 3) which closely matched those found when using Soltrol-130 in glass columns (Wilson et al., 1988). This result suggests that the differences in residual saturation values were related not to differences in fluid characteristics, but to the amount of time the liquid/soil system had in which to equilibrate.

The wettability of the column walls was also found to affect the amount of time required to reach an equilibrium during the organic liquid flood. That is, how well an organic liquid wetted the column side wall affected how the liquid traveled through the column. TFE, which formed the walls of the column in these styrene experiments, was preferentially wet by the organic phase.

In an attempt to study a non-wetting phase front advance in the TFE columns, an experiment was conducted in which only one-third of a pore volume of styrene was introduced into a water-saturated TFE column. The experiment was halted at that point and the column was heated to polymerize the styrene. When the column was dissected, all the styrene was found around the edges of the sand-pack in contact with the column walls or endcaps (see Figure 11b). The central core of the

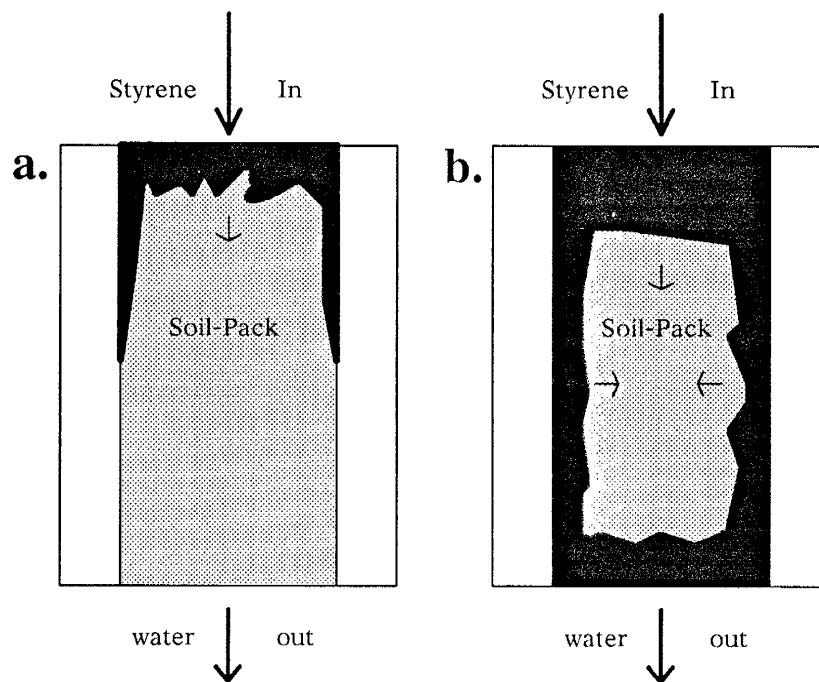


Figure 11. Cross-section of styrene flooding into a water-saturated column with organic wet walls: early time on left, late time on right.

sand-pack had not yet been contacted by styrene. This result indicated that because styrene wet TFE, but not the sand, the advancing styrene followed the walls preferentially (see Figure 11a). Subsequent drainage of water from the center of the column was slowed because the styrene had already achieved a high saturation at the bottom of the column, interfering with water drainage. Due to the time constraints imposed on the styrene experiments, the slower drainage of water resulted in lower maximum organic saturations which contributed to lower residual saturations.

If this non-uniform displacement was typical for styrene, it is probable that the resulting spatial distribution of polymerized styrene blobs may not faithfully simulate the residual organic distributions in the field. This problem is another reason why statistical analyses of blob size and shape using blob and pore casts may be premature for unconsolidated soils. Another column design, such as the glass chromatographic columns used by Morrow et al. (1988) and Wilson et al. (1988) would have walls which are not wet by the organic fluid. Propagation of a non-wetting fluid through the glass column would not be influenced by the phenomenon described above.

At the beginning of this project, we anticipated taking pore casts and performing a size and shape analysis. Such analyses have been conducted on blob casts taken from oil reservoir sandstone cores and glass bead packs by our colleagues here at New Mexico Tech's Petroleum Recovery Research Center (Morrow and Chatzis, 1982, Chatzis et al., 1983, and Chatzis et al., 1988). As discussed previously, the pore casts taken from the Sevilleta soil columns appeared to be too fragile for quantitative analysis using a Coulter Counter or even an image analyzer. Many of the larger casts broke into several pieces when handled. The right end of the blob cast depicted in the lower right photo of Figure 8 is broken. This complex blob of roughly 15 pore bodies was even bigger before it broke. The branched blob in the lower left also appears to have broken ends. Breakage of this kind

would have severely biased a size analysis. It is possible that the PRRC samples also suffered from the same problem, and their results may be so biased. A second approach would be to use image analysis on the sectioned epoxied pore casts. This proved beyond the resources of this project, but is strongly recommended in future research efforts.

Figure 9 is a photomicrograph of a Sevilleta sand pore cast, showing many blobs. The blobs appear light blue and the wetting phase appears yellow-orange. Figure 10 is SEM photomicrograph of a random sample of Sevilleta blob casts. The pore cast shows that, in the saturated zone, non-wetting fluids are trapped in the center of pores and pore throats, never touching the soil grains. These photographs also indicate that most of the Sevilleta blobs are larger than a singlet or doublet. Upon closer inspection of the pore cast, with a stereoscope, it is seen that most of the blobs, which appear on the surface to occupy only one or two pores, actually extend down into the sample. Blobs commonly wind down and around into the pore network forming 'ghosts' at depth when viewed through the relatively transparent quartz sand. Figure 10 may be somewhat misleading in reference to the size of the blobs. Although it shows a good percentage of singlets and doublets, it must be remembered that many of the blob casts in the photomicrograph are broken.

Inspection of Heterogeneous Sand Packs

Figures 12 and 13 are photographs showing the results of capillary trapping of the organic liquid at the end of heterogeneous experiments 1 and 2. Water was flooded from the left of the picture to the right in order to mobilize, or trap, the styrene. Note the thin line of connected styrene filled pores at the up-gradient end of the heterogeneity in Figure 13. High organic saturations (see S_o column in Table 3) indicate that the organic liquid displaced the aqueous phase from the larger pores found in the stringers. This was expected, as a non-wetting fluid will move preferentially to larger pores in order to decrease its surface to volume ratio, and therefore decrease the surface energy of the system. So with the larger pores available, more non-wetting liquid can enter the system for a given energy level, or head. The fact that the columns were packed dry may have also contributed to the higher S_o values seen in these experiments (0.9 vs. 0.7). The dry soil may have settled and compacted during the water saturation process, creating a large pore at one end of the column. This one 'macro' pore could have filled with styrene and contributed to a high organic saturation.

The S_{or} values presented in the last column of Table 3 represent 'bulk' residual saturations in that they are averaged over the whole heterogeneous column. Observations of the core, after it had been cut on a rock saw indicate however, that most of the residual styrene was trapped in the coarse stringers. A lesser amount, approximately the same as that observed in the earlier homogeneous experiments (16%), was trapped in the finer matrix. If one assumes that little to no drainage of styrene occurred in the stringers, the measured 'bulk' residual saturation in Table 3 can be compared with a theoretical value:

$$\begin{aligned} \text{Estimated bulk residual styrene saturation} &= \\ &= (\textit{normalized lens volume}) \times S_o + (\textit{normalized matrix volume}) \times S_{or} \\ &= (0.40 \times 0.90) + (0.60 \times 0.16) = (0.36 + 0.09) = 0.45 = 45\% \end{aligned}$$

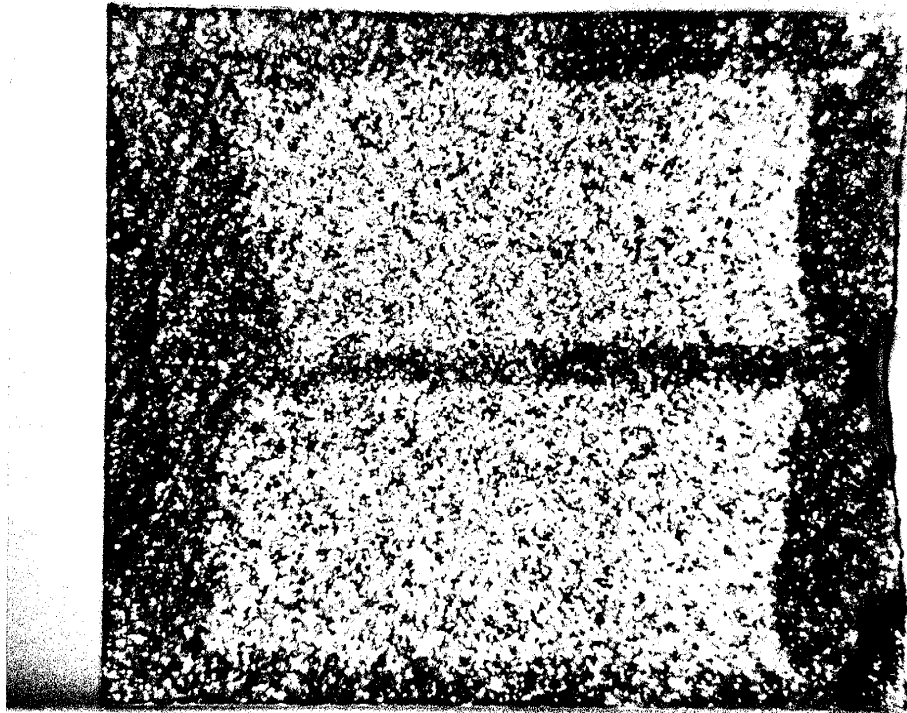


Figure 12. Photograph of heterogeneous sand pack. Water was flooded from left to right at a low rate. The core is 5 cm long.

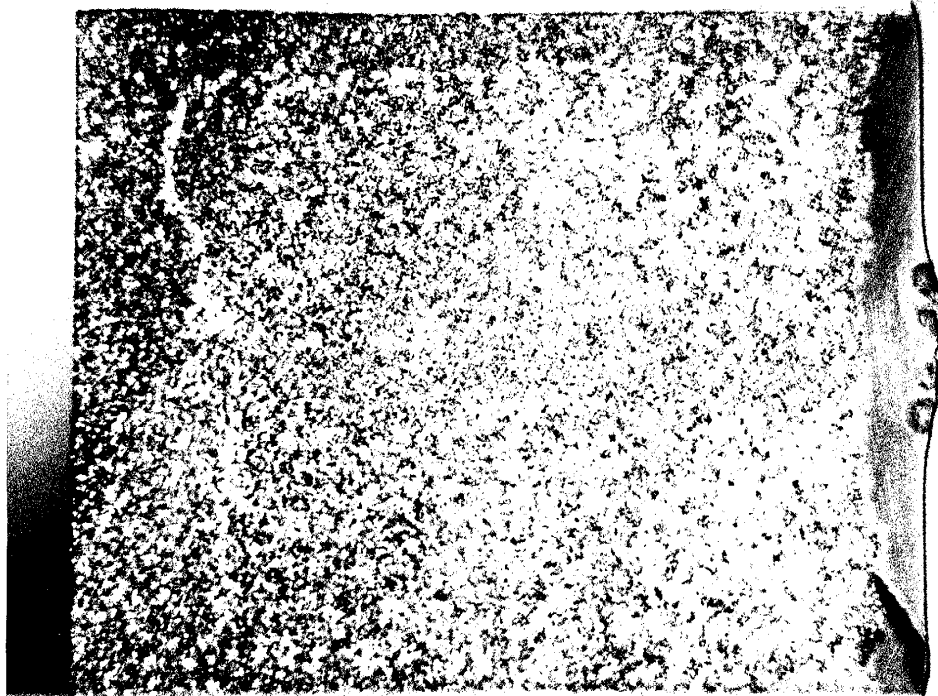


Figure 13. Photograph of heterogeneous sand pack. Water was flooded from left to right at a high rate. The core is 5.8 cm long.

Column 1's value of residual saturation, 41%, comes close to the theoretical value while column 2 is nowhere near the predicted value. This suggests that by-pass trapping may not totally exclude water from the coarse stringers.

The differing S_{or} values of experiments 1 and 2 are explained by the flow rate of the water flood. Column experiment 1 (Figure 12) was water-flooded at a much lower rate than column 2, approximately 1 ml/minute, and was oriented vertically; the water flowed from the bottom to the top. Buoyancy forces were helping to move the less dense styrene upward and out of the column. The flow was controlled by pushing water through the column with a syringe pump. The low flow rate led to a situation where almost 45% of the styrene in the column was bypassed and trapped. In this case, the combination of viscous and buoyancy forces were not strong enough to overcome the capillary forces holding the styrene in place. Although some CaCl_2 did flow through the stringers, the majority of the stringer's pore space remained filled with styrene. Experiment 1 (Figure 13), in contrast, was flooded with water as described in the water flood section of this paper. It had a maximum flow rate of 100 ml/minute, two orders of magnitude greater than the flow rate in 2. Also, the column was oriented so that its long axis (i.e. the flow direction) was horizontal, effectively negating any buoyancy effects. All the styrene removed from the column was mobilized by viscous forces. The residual saturation value, 26%, as well as visual inspection of the column, indicated that the styrene had been pushed out of the coarse stringers by the water. Well connected styrene still remained in the last half of the down gradient end of the stringer but the rest was reduced to small disconnected blobs.

The above results imply that at low flow rates, in the Sevilleta sand, capillary forces in the coarse stringers are dominant over the combination of buoyancy and viscous forces. At some flow rate, between 1 ml/min and 100 ml/min, mobilization of the styrene trapped in the stringers would begin; this is obvious from the results of experiment 2. Whether the mobilization, or flushing, of the styrene behaves somewhat linearly with respect to water velocity, or whether there is a sudden increase in mobilization at a single water velocity, requires more study. The fact that some styrene has been displaced from the stringers, as seen in Figure 12 and as estimated with the bulk residual saturation, argues for the 'somewhat linear' behavior. The evidence is, however, not definitive. These results do suggest that trapping in the field, due to heterogeneities, can be overcome with high enough flow rates. Whether or not these flow rates are practical for field recovery of organic liquids remains to be seen.

Unsaturated Zone Experimental Results

The distribution of the trapped fluids in the vadose zone is markedly different from the distribution found below the water table. Figure 14 is a photomicrograph of a glass bead pack (1 mm bead diameter) showing drained wetting and intermediate-wetting phases. Light blue styrene represents the wetting (water) phase and red dyed Tra-Bond® 2114 represents the intermediate-wetting (organic) phase. The non-wetting (air) phase has not been replaced by epoxy. In this photomicrograph the fluids are distributed almost ideally on and around the beads. Styrene appears as pendular rings at bead contacts and as blue (lower left) coatings upon the bead surfaces. Drained wetting phase distributions have been described previously by Hillel (1980), Gvirtzman et al. (1987) and others. The Tra-bond

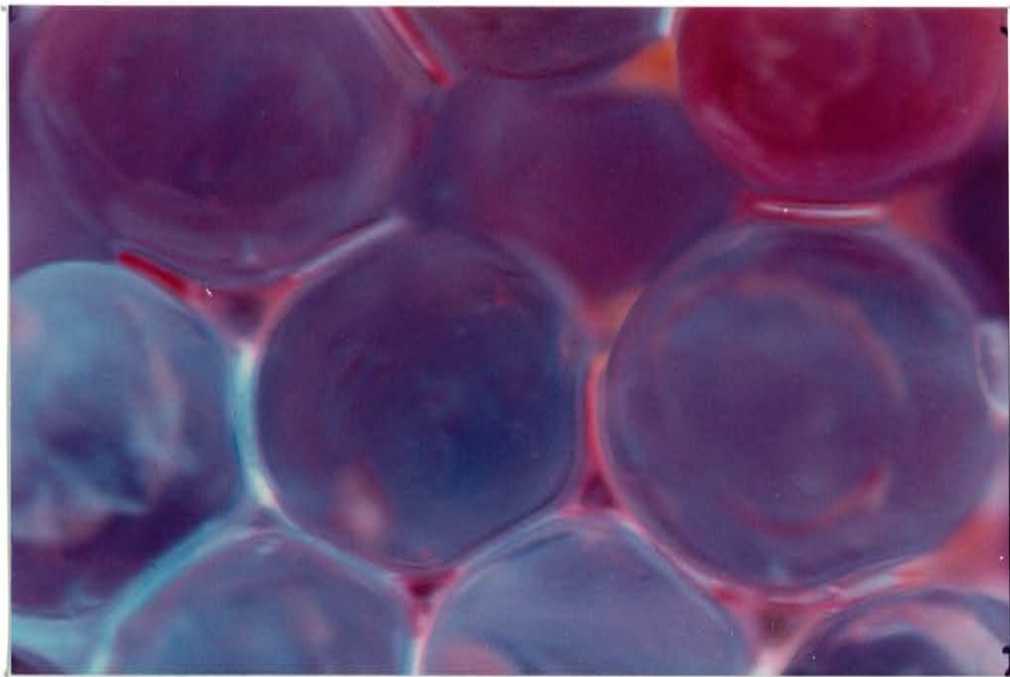


Figure 14. Photomicrograph of drained wetting and drained intermediate-wetting phases in a glass bead pack. Beads are 1 mm in diameter



Figure 15. Photomicrograph of three-phase system. On the overlay 'w' stands for wetting phase, 'I' stands for intermediate wetting, 'N' stands for the non-wetting phase, and 'G' stands for grain. Note the well drained pore. Sample is magnified 100 times

occurs as thin films, again coating the beads, partially covering the styrene pendular rings, and also coating pore interiors. This is similar to the conditions described by Salathiel (1973) and Schuille (1984, 1988). The intermediate-wetting phase can also be seen forming a pendular ring, next to a pore from which the epoxy drained, in the upper left corner of the Figure. This mixture of intermediate-wetting and wetting phenomenon begins to hint at the complexities of natural systems. This bead pack, after all, provides a system of uniform, well rounded, well packed grains, something not commonly found in nature.

Natural systems, as presented in Figure 15, yield a more complex picture. This photomicrograph shows an unpolished pore cast surface of a three phase experiment which was performed using the Sevilleta sand. Styrene appears as fuzzy blue patches on grains and at grain contacts. One can infer that these are thin films and pendular rings but the photo does not actually show the wetting relationships as well as Figure 14. The intermediate-wetting epoxy is light pink and occurs between the wetting and non-wetting phases. It is also found filling pores from which it failed to drain. The non-wetting phase is green and fills the center of pores which have been drained of the intermediate-wetting phase. Sand grains appear dark pink in color and are generally more opaque than the epoxies. Figure 16 is a schematic of a cross section through a three-phase soil column. The ideal drainage of the intermediate-wetting epoxy, as depicted in Figure 14 and 16, is visible in one pore in Figure 15. The pore is formed by the conjunction of three sand grains. Styrene occurs as pendular rings at the grain contact points. Immediately next to the wetting pendular rings are small pockets of the intermediate wetting phase. It is obvious that the pink epoxy is wetting relative to the green non-wetting phase, which is found at the center of the pore.

It is obvious that the majority of the pores in the photomicrograph, however, are showing non-ideal behavior. Several pores remained totally filled with the intermediate-wetting phase. It seems likely that the undrained pores of the intermediate-wetting phase are an artifact of the rapid draining procedure. The relatively high viscosity (50-60 cps) and rapid setup of the Tra-Bond epoxy required greater flow rates and higher pressures in the column. Higher pressures caused air to break through the Durapore® filter, effectively stopping the epoxy drainage. The polyvinylidene difluoride filter allowed approximately 50% of the intermediate-wetting epoxy to be drained, but the other 50% was left totally undrained, or by-passed. Flooding the column with the third phase showed that air followed the edge of the sand pack downward, between the column wall and the sand, and contacted the filter. A similar problem occurred with the glass bead pack, but better drainage of the was effected using only a fritted glass disk as a capillary barrier. The higher permeability of the large (1 mm diameter) beads made this feasible. In an attempt to improve the epoxy drainage of the sand pack another low viscosity epoxy, Polysciences' Ultralow® ($\nu = 10$ cps), was tried but the epoxy proved to be incompatible with the already hardened styrene. The Ultralow leached the 9,10-diphenylanthracene dye out of the styrene and made it impossible to distinguish between the two phases.

In addition to the air breakthrough problem, the Tra-bond epoxy may also have drained preferentially through macropores, or pore pathways with a larger average diameter and lower aspect ratio. Large amounts of the epoxy would have been by-passed and trapped if this were the case. Multi-pore blobs, retrieved from the two phase systems (Figures 8 and 10), suggest that pore body-pore throat aspect ratios can be close to one; keeping in mind that the saturated zone blobs are

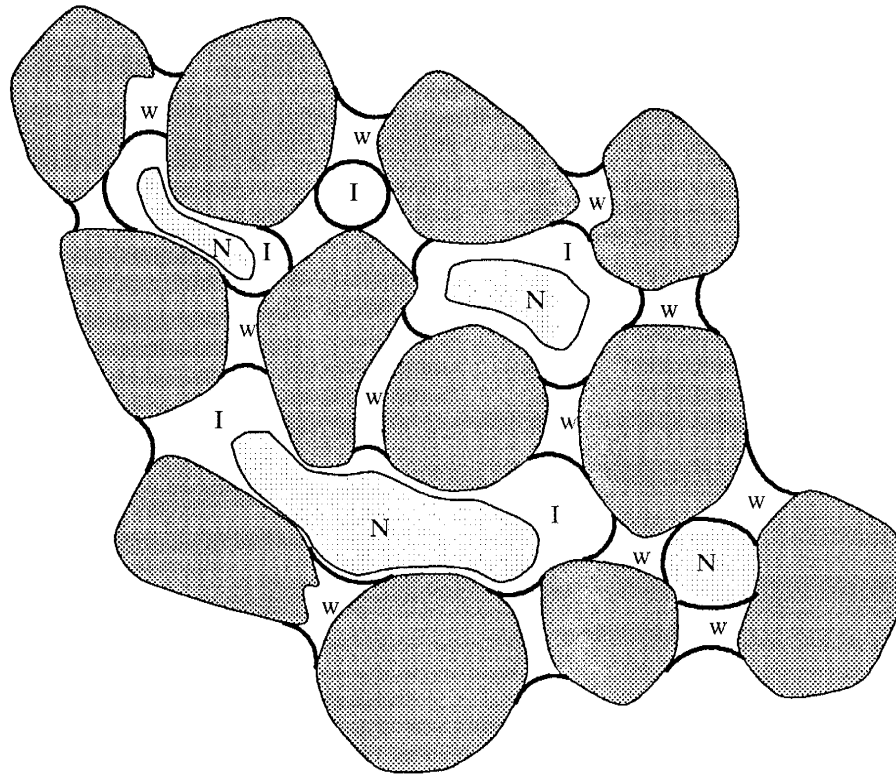


Figure 16. Schematic cross-section through a coarse grained soil. W stands for the wetting phase; I stands for the intermediate wetting phase; N stands for the non-wetting phase.

a muted representation of the pore topology. Though the Sevilleta sand is very uniform, its grains are sufficiently different so that macropores, created during the packing process should not be ruled out.

Another difficulty with the system as shown in Figure 15 is that the volume of the wetting phase, visible as pendular rings, seems much too small. The seeming lack of the wetting phase can be explained by considering the shapes of the sand grains; they are sub-angular. A pendular ring will form at the contact between two grains when liquid is trapped by capillary forces, at and around the contact, as it drains. The larger the radii of curvature of the two touching grains are, the larger the pendular ring will be. It follows then that a drained wetting fluid will form larger pendular rings on large, round glass beads than on smaller, angular sand grains. It is obvious that the two most prominent pendular rings, visible in Figure 15, occur at grain contacts on a long flat sand grain, with a large radius of curvature. Other pendular rings are probably just too small to be seen or are covered by the intermediate-wetting phase.

CONCLUSIONS

The objective of this study was to simulate multi-phase fluid distributions, at residual oil saturations, using styrene monomer and epoxy resins. Styrene simulates organic liquids immiscible

with water very well. Its viscosity, which increases over time, is its one drawback. This drawback leads to difficulties when trying to perform quantitative displacement experiments but has little effect on the use of styrene for saturated zone flow visualization. Styrene also works well to simulate wetting liquid distributions, such as the water phase in three phase experiments. It must be remembered that styrene will not polymerize in the presence of oxygen so another gas, nitrogen for example, must be used as the non-wetting gas phase.

In saturated zone displacement experiments with immiscible fluids, we found that column-fluid wettability relationships affect the observed results. The organic wet TFE walls of the experimental column allowed the styrene, while acting as a non-wetting fluid, to by-pass the water wet sand core, leading to decreased S_o (or increased S_{wi}) values. If enough time was allowed for the system to approach equilibrium, this effect was negated.

The study of blob and pore casts indicated that, in the saturated zone, trapped non-wetting liquids form a variety of shapes: from singlets occupying one pore to complex, branching multi-pore blobs. These trapped blobs occupy the center of the pores and pore throats. Non-wetting liquids trapped in the vadose zone are distributed much differently than those trapped in the saturated zone. The intermediate-wetting organic liquid forms thin films over grain surfaces and totally fills pores, at least for the interfacial tensions tested.

Studies of heterogeneous sand packs showed that at aquifer flow rates, heterogeneities in soils strongly affect trapping of non-wetting liquids below the water table. Non-wetting fluids preferentially fill larger pores. Water, moving at a low flow rate, will by-pass these larger pores leaving large amounts of the non-wetting phase behind. At higher flow rates the wetting phase can mobilize the non-wetting phase trapped in larger pores, decreasing the bulk residual saturation.

REFERENCES

- Adamson, A. W.** 1982. *Physical Chemistry of Surfaces*, 4th edition. Wiley, New York.
- Amaufule J. O., and L. L. Handy.** 1982. The effect of interfacial tensions on relative oil/water permeabilities of consolidated porous media. *SPE Journal*, vol.22, no.3, pp.371-381.
- ASTM.** 1986. *Annual Book of ASTM Standards*. American Society for Testing and Materials, Philadelphia, PA.
- Boyer, R. F., ed.** 1970. Styrene Polymer, in *Encyclopedia of Polymer Science and Technology* (Bikales, N. M., ed.), vol.13, Interscience Publishers, New York, pp.128-447.
- Burmester, D. E., and R. H. Harris.** 1982. Groundwater contamination: an emerging threat. *Technology Revue*, vol.84, no.7, pp.50-62.
- Chaffee, W. T., and R. A. Weimar.** 1983. Remedial programs for ground-water supplies contaminated by gasoline. Third National Symposium on Aquifer Restoration and Ground-Water Monitoring, National Water Well Association, pp.39-46.
- Chatzis, I., N. R. Morrow, and H. T. Lim.** 1983. Magnitude and detailed structure of residual oil saturation. *SPE Journal*, vol.23, no.2, pp.311-25.
- Chatzis, I., M. S. Kuntamukkula, and N. R. Morrow.** 1984. Blob-size distribution as a function of capillary number in sandstones. paper SPE 13213, presented at 1984 SPE Annual Technical Conference and Exhibition, Houston, TX.
- Chatzis, I., M. S. Kuntamukkula, and N. R. Morrow.** 1988. Effect of capillary number on the microstructure of residual oil in strongly water-wet sandstones. *Soc. Pet. Eng. Reservoir Engineering*, vol.3, no.3, pp.902-912.
- Convery, M. P.** 1979. The Behavior and Movement of Petroleum Products in Unconsolidated Surficial Deposits. M.S. Thesis, University of Minnesota.
- Feenstra, S., and J. Coburn.** 1986. Subsurface contamination from spills of denser than water chlorinated solvents. *Bull. Calif. Water Poll. Control Assoc.* vol.23(4), pp.26-34.
- Gvirtzman, H., M. Magaritz, E. Klein, and A. Nader.** 1987. A scanning electron microscopy study of water in soil. *Transport In Porous Media*, no.2(1987), pp.83-93.
- Hillel, D.** 1980. *Fundamentals of Soil Physics*. Academic Press, New York, NY, 413p.
- Jercinovic, D. E.** 1984. Petroleum-Product Contamination of Soil and Water in New Mexico. Ground Water/Hazardous Waste Bureau, New Mexico Environmental Improvement Division, EID/GWH-84/4.
- Maugh II, T. H.** 1979. Toxic waste disposal a growing problem. *Science*, vol.204, pp.819-23.

- McKee, J. E., F. B. Lavery, and R. H. Hertel.** 1972. Gasoline in groundwater. *Journal of the Water Pollution Control Federation*, vol.44, no.2, pp.293-302.
- McKellar, M., and N. C. Wardlaw.** 1988. A Method of Viewing "Water" and "Oil" Distribution in Native-State and Restored-State Reservoir Core. *AAPG Bulletin*, V. 72, No. 6 (June), pp. 765-771.
- Morrow, N. R., and I. Chatzis.** 1982. Measurement and Correlation of Conditions for Entrapment and Mobilization of Residual Oil. Report DOE/BC/10310-20, Department of Energy.
- Morrow, N. R.** 1984. Measurement and Correlation of Conditions for Entrapment and Mobilization of Residual Oil. Report NMERDI 2-70-3304, New Mexico Energy Research and Development Institute, Santa Fe, NM.
- Morrow, N. R., I. Chatzis, and J. J. Taber.** 1988. Entrapment and mobilization of residual oil in bead packs. *SPE Reservoir Engineering*, vol.3, no.3, pp.927-934.
- Salathiel, R. A.** 1973. Oil recovery by surface film drainage in mixed-wettability rocks. *Journal of Petroleum Technology*, vol.25, pp.1216-24.
- Schwille, F.** 1984. Migration of organic fluids immiscible with water in the unsaturated zone. in *Pollutants in Porous Media: The Unsaturated Zone Between Soil Surface and Groundwater* (B. Yaron, G. Dagan, and T. Goldschmid — eds.), Springer-Verlag, New York, pp.27-48.
- Schwille, F.** 1988. *Dense Chlorinated Solvents in Porous and Fractured Media*. Lewis Publishers, Chelsea, MI. 146pp.
- Weast, R. C. (ed.).** 1981. *Handbook of Chemistry and Physics*. CRC Press, Boca Raton, Fla.
- Wilson, J. L., S. H. Conrad, E. Hagan, W.R. Mason, and W. Peplinski.** 1988. The pore level spatial distribution and saturation of organic liquids in porous media. in proceedings of *Petroleum Hydrocarbons and Organic Chemicals in Ground Water*, NWWA, Houston, TX, pp.107-133.
- Wilson, J. L., S. H. Conrad, W. R. Mason, W. Peplinski, and E. Hagan.** 1989. Laboratory investigation of residual liquid organics from spills, leaks, and the disposal of hazardous wastes in ground water *U.S. EPA Report*, R. S. Kerr Laboratory, Ada, Oklahoma, (in press).
- Yadav, G. D., F. A. L. Dullien, I. Chatzis, and I. F. Macdonald.** 1987. Microscopic Distribution of Wetting and Nonwetting Phases in Sandstones During Immiscible Displacements. *SPERE* (May, 1987), pp. 137-147.